JOURNAL OF GAS TECHNOLOGY

Volume 9 / Issue 2 / Winter 2024 / Pages 70-87

Journal Home page: http://jgt.irangi.org

# The Impression of Roughness on Flow Pattern and Performance of Axial Gas Cyclone Along with Erosion Rate

**Masoud Dorfeshan[1*], Sattar Moghaddam[2], Farzad Parvaz[3]**

1. Assistant Professor, Department of Mechanical Engineering, Faculty of Engineering, Behbahan Khatam Alanbia University of Technology, Behbahan, Iran
2. M.Sc. Student, Department of Mechanical Engineering, Faculty of Engineering, Behbahan Khatam Alanbia University of Technology, Behbahan, Iran
3. M.Sc., Department of Mechanical Engineering, Semnan University, P.O. Box 35131-191, Semnan, Irann

## ARTICLE INFO

ORIGINAL RESEARCH ARTICLE

**Article History:**
Received: 14 November 2024
Revised: 19 December 2024
Accepted: 30 December 2024

**Keywords**:
Axial gas cyclone
Wall roughness
Pressure drop
Wall erosion
Discrete phase model

## ABSTRACT

In this study, the effect of wall roughness on flow pattern, performance, and erosion rate in an axial gas cyclone is investigated. Gas cyclones are widely used in various industries such as food processing, dryers, and the cement industry for separating solid particles from gas flow due to their flexibility, low maintenance costs, and efficiency in air pollution control. Numerical modeling is conducted using turbulence models, surface roughness models, the discrete phase model (DPM), and the erosion model to analyze key parameters such as pressure drop, tangential velocity, axial velocity, separation efficiency, and wall erosion rate. The results indicate that increasing wall roughness reduces tangential velocity, thereby decreasing centrifugal force, which negatively affects particle separation efficiency. On the other hand, increasing wall roughness leads to a reduction in pressure drop, which is considered an advantage in cyclone design. Erosion rate analysis also shows that the highest erosion occurs in the lower conical section of the cyclone, and increasing wall roughness can reduce erosion. Overall, this study reveals that wall roughness has conflicting effects on cyclone performance—reducing pressure drop on one hand while decreasing separation efficiency on the other. Therefore, optimizing surface roughness is essential to achieve a balance between these two factors in the design of axial gas cyclones. The results showed that increasing wall roughness reduced tangential velocity by up to 18%, cyclone collection efficiency dropped by approximately 12% for particles larger than 25 μm, while pressure drop decreased by around 9%, which can be considered beneficial in energy-sensitive applications. The highest erosion rate was observed at the cone tip of the cyclone, and wall roughness helped reduce average erosion by nearly 15%.

DOR: 20.1001.1/jgt.2025.2057137.1054

**How to cite this article**
M. Dorfeshan, S. Moghaddam, F. Parvaz, The Impression of Roughness on Flow Pattern and Performance of Axial Gas Cyclone Along with Erosion Rate. Journal of Gas Technology. 2024; 9(2): 70 -87. ( https://www.jgt.irangi.org/article_726453.html )

* Corresponding author.
E-mail address: dorfeshan@bkatu.ac.ir, (M. Dorfeshan).

Available online 30 December 2024

## 1. Introduction

Gas cyclones are widely utilized across various industries to separate solid particles from airflow. Due to their flexibility, low maintenance costs, and effectiveness in air pollution control, these devices have gained significant attention from researchers and engineers. They are extensively applied in industries such as food processing, drying, and cement production. Gas cyclones operate based on centrifugal force, classifying solid particles according to their size or density. With advancements in computational technologies, commercial software has become instrumental in modeling complex flow patterns. Numerous studies have adopted numerical approaches to analyze gas cyclone performance (Vahedi et al., 2020; Parvaz et al., 2017; Vahedi et al., 2018; Vahedi et al., 2017; Parvaz et al., 2018; Parvaz et al., 2023; Dehdarinejad et al., 2023; Foroozesh et al., 2021; Babaoğlu et al., 2021; Elsayed et al., 2020; Babaoğlu et al., 2018; Parvaz et al., 2020; Parvaz et al., 2023). Among different types of gas cyclones, conventional gas cyclones and axial gas cyclones (AGCs) are commonly used for particle separation. The primary distinction between these two types lies in the direction of the gas stream, which is categorized into tangential inlets and guide vanes (Mao et al., 2019; Zhang et al., 2021). Both configurations facilitate gas flow within the cyclone. AGCs, as well as conventional gas cyclones, are widely employed in industrial applications to achieve high separation efficiency with minimal cost. Additionally, axial gas cyclones can be further classified into subcategories such as one-through gas cyclones, uniflow separators, and swirl flow separators (Austrheim, 2006). Compared to axial gas cyclones, these variants are generally smaller in size. While certain designs can reduce pressure drop, they often result in lower collection efficiency compared to axial gas cyclones (Austrheim, 2006; Deng et al., 2020). Notably, in AGCs, both gas flow and solid particles follow the same trajectory (Hsiao et al., 2011; Li et al., 2020), and the outlet for both the duty gas and clean gas is located at the same end. Extensive research has been conducted on the operation, design, and optimization of axial gas cyclones (Li et al., 2023; Elsayed and Lacor, 2010). Studies have focused on improving AGC performance by investigating geometric parameters, including the shape of guide vanes (Austrheim, 2006; Brar and Elsayed, 2018), the separator body (Elsayed et al., 2020; Brar and Elsayed, 2017), and the dimensions of the outlet tube (Brar et al., 2015). Ogawa et al. (1997) conducted both experimental and numerical studies on axial gas cyclones, evaluating axial velocity, tangential velocity, pressure drop, and cut-off diameter. However, their simulations exhibited slight deviations, particularly in total collection efficiency. In an effort to enhance AGC performance, Hsu et al. (2005) designed a novel guide vane for an axial separator dust collector operating under low-pressure conditions. Furthermore, they introduced three outlet tubes in an axial gas cyclone to compare AGC performance with conventional gas cyclones. Their findings indicated that a funnel-shaped outlet tube could enhance AGC performance, although pressure drop did not exhibit a direct correlation with funnel diameter. Similarly, Hsiao et al. (2011) investigated various geometric modifications, such as vortex finder length and an inverted cup structure, to predict AGC performance relative to conventional gas cyclones. Their results demonstrated that incorporating an inverted cup in AGCs could improve collection efficiency while reducing pressure drop. Further optimizations have been explored by Xiong et al. (2014), who analyzed the shape of the vortex finder, revealing that incorporating a helical gap and a reflex cone could enhance collection efficiency. Zhang et al. (2021) proposed a novel approach for determining the empirical constant introduced by Hsu et al. (2005), achieving strong agreement with experimental data. Additionally, Huang et

al. (2018) numerically examined the influence of geometric parameters on AGC performance. Their findings indicated that the torsion angle and exit angle of the vanes significantly impact both pressure drop and collection efficiency. Moreover, they investigated body diameter variations to determine the relationship between axial and tangential velocity and pressure drop. Gopalakrishnan et al. conducted numerical studies on pressure drop and collection efficiency in axial gas cyclones with axial inlets. They examined the influence of guide vane configurations on AGC performance, identifying that the number and angle of blades play a crucial role in enhancing collection efficiency. In this study, a simulation-based approach is employed to investigate the complex physical flow within an axial gas cyclone with high accuracy. Initially, the continuity phase is simulated using the k-ε turbulence model to establish preliminary convergence. Once all equations converge, the Reynolds Stress Model (RSM) is selected due to its capability of capturing detailed flow behavior within the gas cyclone, despite its relatively slow convergence compared to other turbulence models. Furthermore, the one-way coupling method is utilized to track suspended particles inside the axial gas cyclone. This study also examines the flow pattern and performance of gas cyclones, emphasizing the impact of wall roughness and erosion phenomena. Notably, the guide vanes, a crucial component of axial gas cyclones, play a significant role in enhancing collection efficiency.This revision improves the clarity, formality, and coherence of the text, making it more suitable for a scientific article. Recent works have emphasized the role of surface treatments and material engineering in enhancing cyclone performance. For instance, Li et al. (2024) demonstrated that surface coatings significantly influence wall erosion and flow stability. Similarly, Rahimi and Singh (2025) introduced a geometry-based optimization approach to improve both separation efficiency and mechanical durability in axial gas cyclones.

## 2. Governing Equations

### 2.1. Turbulent Model

Previous studies on gas cyclones have demonstrated that selecting an appropriate turbulence model is crucial for achieving high accuracy, as the airflow into gas cyclones exhibits significant swirl and strain. This suggests that the RSM model is more effective than the two-stage model (Dehdarinejad et al., 2023; Babaoğlu et al., 2021; Elsayed et al., 2020).

$$\frac{\partial \overline{u_i}}{\partial x_i} = 0 \tag{1}$$

$$\frac{\partial \overline{u_i}}{\partial t} + \overline{u_j}\frac{\partial \overline{u_i}}{\partial x_j} = -\frac{1}{\rho}\frac{\partial \overline{P}}{\partial x_i} + \nu\frac{\partial^2 \overline{u_i}}{\partial x_i \partial x_j} - \frac{\partial}{\partial x_j}R_{ij} \tag{2}$$

Where $\overline{u_i}$ is the mean velocity vector, xi is the position vector, $\overline{P}$ is the mean pressure, $\rho$ is the gas density, $\nu$ is the gas kinematic velocity, and $R_{ij} = \overline{u_i' u_j'}$ is the Reynolds stress tensor. Here $u_i' = u_i - \overline{u_j}$ is the ith fluctuating velocity component. The RSM turbulence model provides the transport equations for the evaluation of turbulence stresses. That is,

$$\frac{\partial}{\partial t}R_{ij} + \overline{u_k}\frac{\partial}{\partial x_k}R_{ij} = \frac{\partial}{\partial x_k}\left(\frac{\nu_t}{\sigma^k}\frac{\partial}{\partial x_k}R_{ij}\right) + \left[R_{ik}\frac{\partial \overline{u_j}}{\partial x_i} + R_{jk}\frac{\partial \overline{u_i}}{\partial x_k}\right] - C_1\frac{\varepsilon}{k}\left[R_{ij} - \frac{2}{3}\delta_{ij}K\right] - C_2\left[P_{ij} - \frac{2}{3}\delta_{ij}P\right] - \frac{2}{3}\delta_{ij}\varepsilon \tag{3}$$

Where the turbulence production term $P_{ij}$ is given as,

$$P_{ij} = -\left[R_{ik}\frac{\partial \overline{u_j}}{\partial x_k} + R_{jk}\frac{\partial \overline{u_i}}{\partial x_k}\right], \quad P = \frac{1}{2}P_{ij} \tag{4}$$

Here $P$ stands for the fluctuating kinetic energy production, $\nu_t$ stands for the turbulence (eddy) kinematic viscosity, and the empirical constants are $\sigma^k = 1, C_1 = 1.8, C_2 = 0.8$. The transport equation for the turbulence dissipation rate, $\varepsilon$, is given as,

$$\frac{\partial \varepsilon}{\partial t} + \overline{u_j}\frac{\partial \varepsilon}{\partial x_j} = \frac{\partial}{\partial x_j}\left[\left(\nu + \frac{\nu_t}{\sigma^\varepsilon}\right)\frac{\partial \varepsilon}{\partial x_j}\right] - C^{\varepsilon 1}\frac{\varepsilon}{K}R_{ij}\frac{\partial \overline{u_i}}{\partial x_j} - C^{\varepsilon 2}\frac{\varepsilon^2}{K} \tag{5}$$

where $K = \frac{1}{2}\overline{u_i' u_j'}$ is the fluctuating kinetic energy. The values of constants are $\sigma^{\varepsilon} = 1.3$, $\sigma^{\varepsilon 1} = 1.44$, $\sigma^{\varepsilon 2} = 1.92$.

## 2.2. Surface Roughness Model (SRM)

The factor that affects the airflow resistance and the momentum transmission is the wall roughness of the cyclone. The law of the wall velocity profile near a rough surface is given by (Kaya et al., 2011).

$$\frac{\bar{u}}{u^*} = \frac{1}{k}\ln\left(\frac{yu^*}{\nu}\right) + B - \Delta B\left(k_S^+\right) \quad (6)$$

Where $\bar{u}_i$ is the mean velocity, $y$ is the distance from the wall, $u^*$ the friction velocity, $v$ is the kinematic viscosity, and $k_s^+$ is the non-dimensional surface roughness height. In Equation (6) $k = 0.41$ is the von Karman constant, and $B$ is an empirical constant for smooth walls. The friction velocity is defined by:

$$u^* = \left(\frac{\tau_w}{\rho}\right)^{0.5} \quad (7)$$

Where $\tau_w$ is the wall shear stress and $\rho$ is the fluid density. The roughness function, $\Delta B$, depends on the dimensionless surface roughness, $k_s^+$, which is calculated as,

$$k_S^+ = \frac{k_s u^*}{\nu} \quad (8)$$

In the case of hydro-dynamically smooth flows with $k_s^+ < 2.25$ the roughness function $\Delta B = 0$ The roughness function is given as,

$$\Delta B = \frac{1}{k}\ln\left(1 + C_s k_s^+\right) \quad (9)$$

If the flow is in a fully rough regime ($k_s^+ > 90$),

$$\Delta B = \frac{1}{k}\ln\left(\left(k_S^+ - 2.25\right)/87.75 + C_S k_S^+\right) \times \sin\left[0.4258\ln\left(k_s^+ - 0.811\right)\right] \quad (10)$$

Otherwise, the values of $B = 5.56$ and $C_S = 0.5$ are used.

## 2.3. Discrete Phase Modeling (DPM)

To simulate solid particles in gas cyclones, the solid particles are used in gas cyclone to name discrete phase modeling (DPM) (Liu et al., 2022). So, the interaction of particles was neglected, which would satisfy the statistical model of Euler-Lagrangian. According to Newton's second law, in Lagrangian model can obtain the particle trajectories. All particles are spherical and the gravity and drag force are extracted from the calculation. Therefore, the equation of movement of particles is written as:

$$\frac{d\vec{u}_p}{dt} = \frac{\vec{u} - \vec{u}_p}{\tau_r} + \frac{\vec{g}\left(\rho_p - \rho\right)}{\rho_p} \quad (11)$$

Particle relaxation time $\tau_r$ is written as:

$$\tau_r = \frac{\rho_p d_p^2}{18\mu}\frac{24}{\mathrm{Re}C_D} \quad (12)$$

Where $\overrightarrow{u_p}$ is the particle velocity, $\vec{u}$ is the gas velocity, $d_p$ is particle diameter, $\rho_p$ is the density of the particle, and relative Reynolds is defined as :

$$\mathrm{Re} = \frac{\rho_p d_p \left|\overrightarrow{u_p} - \vec{u}\right|}{\mu} \quad (13)$$

The drag coefficient, $C_D$ for spherical solid particles can be written as :

$$C_D = a_1 + \frac{a_2}{\mathrm{Re}} + \frac{a_3}{\mathrm{Re}^2} \quad (14)$$

Where $a_1$, $a_2$, and $a_3$ are constant that employ several different range of $Re$ given by Morsi and Alexander (Morsi and Alexander, 1972).

## 2.4. Model of Erosion

Erosion on cyclone walls owing to solid particle impact that was developed by Oka et al. (2005) is employed here to predict erosion rate on walls inside gas cyclones.

$$E_R = \sum_{n=1}^{N_P}\frac{E^{(i)}}{A_{face}^{\ i}} \quad (15)$$

Where $E_R$ is the removed mass flux (kg/m²s). To

obtain the erosion rate (kg/s), $E_R$ is integrated over the total area of the cyclone. In Equation (15) erosion rate, $E^{(i)}$, is determined by:

$$E^{(i)} = 1\times10^{-9} E_V \rho_w \dot{m}_P$$
$$E_V = f(a) E_{90} \quad (16)$$
$$E_{90} = L(H_v)^{k_1}\left(\frac{V_P^{(i)}}{V'}\right)^{k_2}\left(\frac{d_P}{d'}\right)^{k_3}$$

where $E_V$ is volumetric erosion, $\rho_w$ is wall density, $\dot{m}_p$ is mass flow rate of particle, $H_v$ is Vickers hardness, $V_P$ is particle impact velocity, $V'$ is velocity fluctuation, $d'$ is standard diameter, $L$ and $k$ are constant, and $f(\alpha)$ is a function of the impact angle that is given by:

$$f(a) = (\sin a)^{n_1}\left[1 + H_v(1-\sin a)\right]^{n_2} \quad (17)$$

The coefficients of Equations (16) and (17) are presented in (Table 1).

**Table 1: Oka Erosion Model Coefficient**

| $n_1$ | $n_2$ | $H_V(GP)$ | $L$ | $a$ | $b$ |
|---|---|---|---|---|---|
| 0.62 | 5.68 | 0.4 | 65 | 0.109 | 1.58 |
| $k_1$ | $k_2$ | $k_3$ | $V'(m/s)$ | $d'(\mu m)$ | |
| -0.12 | 2.22 | 0.19 | 104 | 326 | |

## 3. Solver Setting

### 3.1. Numerical Schemes

In this study, the numerical outlines for the gas stream were extracted by Karagoz and Kaya (2007). They studied the achievement of varied discretization outlines to select the best way to be more accurate in high swirls in the simulation of gas cyclones. (Table 2) shows the best setting, which is used in current work. One of the more accurate outlines was the PRESTO pressure interpolation. To couple velocity and Pressure, the SIMPELC is applied in the simulation of the airflow inside an axial gas cyclone and the numerical result is close to experimental results. Many researchers highly recommended that the QUICK scheme should be employed for momentum equations. The second order upwind outline was selected for the turbulent dissipation rate and turbulent kinetic energy. Also, the first order upwind was determined by the Reynolds stress.

**Table 2: Detail of Numerical Schemes for the Present Study**

| Numerical setting | Scheme |
|---|---|
| Pressure discretization | PRESTO! |
| Pressure velocity couple | SIMPLEC |
| Momentum discretization | QUICK |
| Turbulent kinetic energy | Second Order Upwind |
| Turbulent dissipation rate | Second Order Upwind |
| Reynolds Stress | First Order Upwind |

### 3.2. Geometry & Boundary Condition

Here, three boundary conditions are used to simulate two-phase flow inside an axial gas cyclone: inlet velocity, outlet, and walls. Airflow is incompressible and isothermal and moves 300 $m^3/h$ uniformly. Solid particles inject independently and are carried by a gas flow. The physical characteristics of particles are followed by the concentration and the density of 300 $mg/m^3$ and 2710 $kg/m^3$ respectively. The boundary condition of "reflect" is chosen at all walls of the cylindrical part. Moreover, all walls of axial gas cyclone and collision between solid particles are supposed to be utterly elastic ( $\epsilon = 1$ ) (Gimbun et al., 2005). Also, the boundary condition of " Trap " is chosen at the bottom of the conical part, where all trajectory calculations are completed and the destiny of particles are made according to "Trapping". Furthermore, the exit tube called the vortex finder chooses the outlet, where solid particles can easily escape and the end can calculate collection efficiency and cut of size diameter.

### 3.3. Grid Generation

In the present investigation, gas-particle flow is injected inside a usual axial gas cyclone. In general, the process of separation is related to centrifugal force, namely fine particles separate from coarse particles. Coarse particles move to walls owing to their density more than fine particles and these particles with the help of the gas boundary layer and gravity acceleration slide along the wall to reach the dustbin and trap, however, fine particles with the assistance of lift force escape through the exit tube. (Figure 1) shows different sections of the axial gas cyclone.

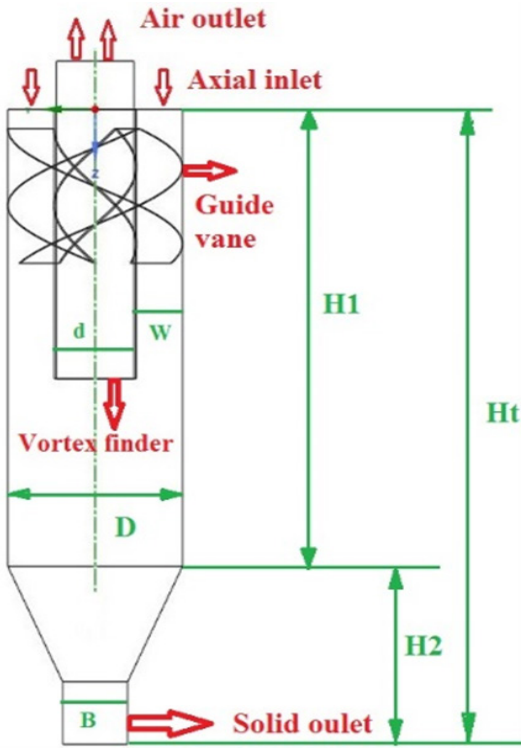


**Figure 1. Different Components of the Axial Gas Cyclone**

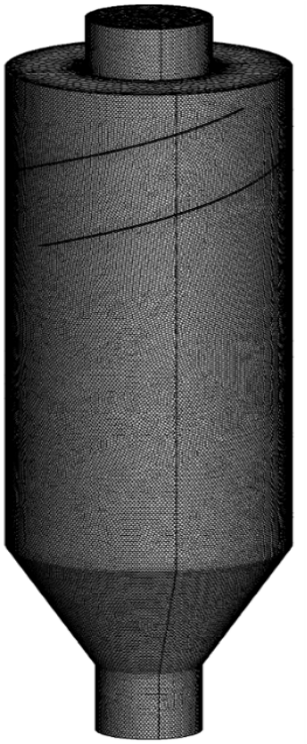

**Figure 2. Structure of the Grids Generated and Used in this Simulation**

Before simulation, meshes are the most significant factor that should be located in the suitable placement of the computational domain. In current numerical simulations, octagonal grids were generated the full domain of axial gas cyclone. (Figure 2) illustrates the shape of the generated grids that are employed in this simulation. For the current axial gas cyclone, the grid independence is investigated by comparing the results of different numbers of cells. (Table 3) shows the variation of cut of size diameter and pressure drop alongside the number of various grids. By comparing their percentage, the best grid was obtained to follow the rest of the simulations.

**Table 3: Details of Grid Independence**

| Cell | Pressure Drop (Pa) | Cut Diameter (micron) |
|---|---|---|
| 827932 | 498250 | 0.5 |
| 956657 | 496496 | 0.6 |
| 1234456 | 497765 | 0.5 |
| Error % | 5.4 | 1.4 |

### 3.4. Validation

In order to validate the present section, the numerical results are first compared with experimental data (Morsi and Alexander, 1972). The numerical results show that with an increase in

velocity for the continuous phase, the air-gas flow inside the axial cyclone experiences an increase in pressure drop. This indicates that this type of cyclone, similar to other gas cyclones, is highly dependent on the velocity or volumetric flow rate of the gas. For the discrete phase, particles ranging from 1 to 40 microns are injected, and the cyclone efficiency is calculated as the ratio of the number of particles released from the cyclone to the total number of particles injected. The results show that as the mass density of the injected particles increases, the efficiency of the cyclone increases, and more particles, compared to smaller ones, are trapped. This is illustrated in (Figure 3).

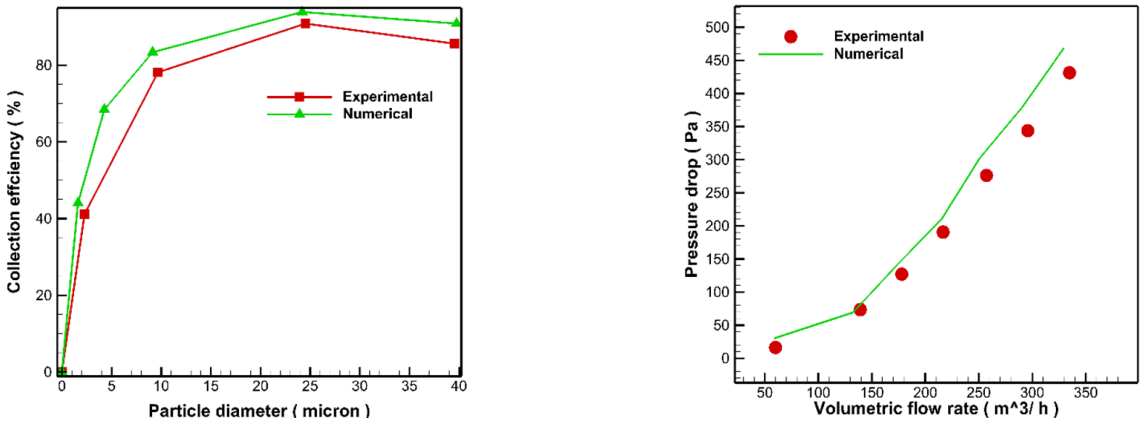


**Figure 3. Validation of the Present Problem**

For validation in the particle erosion section, which is a very important part of the simulation, data from Vera (Oka et al., 2005) for a 90-degree elbow, based on the Okafor model, have been simulated. The numerical results for particle sizes of 150 microns and 300 microns at different velocities, with averaging over the surface of the 90-degree elbow, have been evaluated and are shown in (Figure 4). The graph illustrates the relationship between inlet velocity and maximum erosion rate for two particle sizes (150 µm and 300 µm), based on both experimental and numerical data. As shown, the erosion rate increases with inlet velocity for both particle sizes, with the 300 µm particles exhibiting significantly higher erosion rates compared to the 150 µm particles. Furthermore, the numerical results align well with the experimental data, demonstrating the reliability of the simulation model in predicting erosion behavior under varying flow conditions.

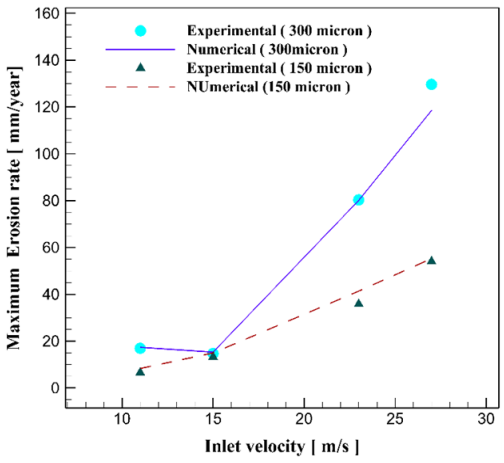


**Figure 4. Validation of the Particle Erosion Section in a 90-Degree Elbow**

As shown in (Figure 5), the highest erosion occurs at the critical angle, approximately 45 degrees, of the 90-degree elbow. The reason for this increase in particle erosion on the 90-degree elbow is that the farther the particles are from the center of curvature, the higher their acceleration and angular velocity. Consequently, the centrifugal force increases, leading to more frequent contact of the particles with the wall, especially at the 45-degree angle, which experiences the highest erosion.

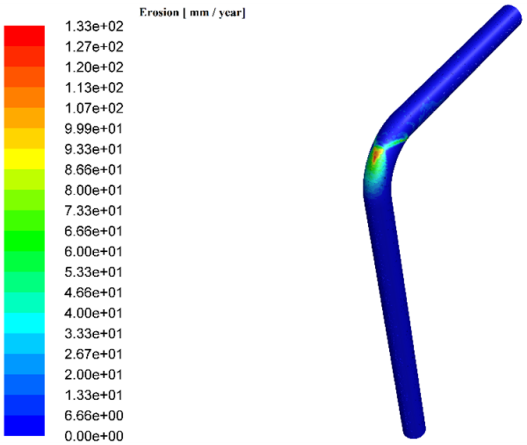


**Figure 5. Particle Erosion Behavior in a 90-Degree Elbow**

## 4. Results

### 4.1. Pressure Drop

When gas enters a cyclone, it forms a boundary layer along the inner wall due to rotational motion. This interaction between the gas and wall surface is the primary source of pressure loss. (Figure 6) shows that wall roughness influences this boundary layer by reducing momentum near the walls, thereby decreasing the pressure drop. As shown in (Figure 7), higher surface roughness consistently lowers the pressure differential between the inlet and outlet.

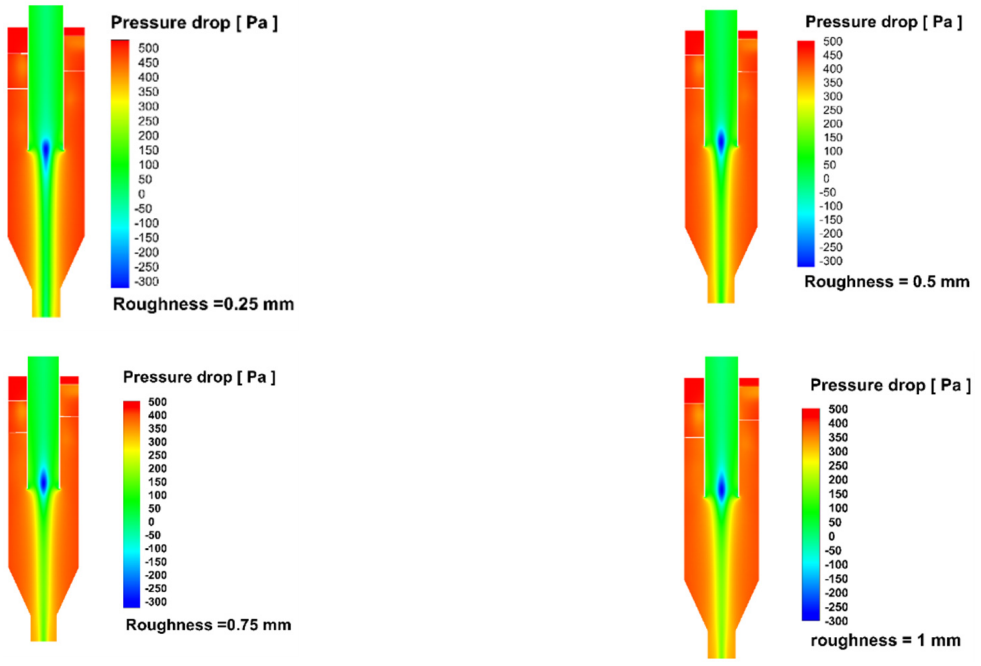


**Figure 6. Pressure Drop Contours with Different Roughness at a Volumetric Flow Rate of 58.95 m²/s**

This effect is particularly valuable in energy-sensitive applications where minimizing pressure loss is critical. In this section, we focus solely on the aerodynamic implications of surface texture, while its influence on efficiency and erosion is discussed in relevant sections.

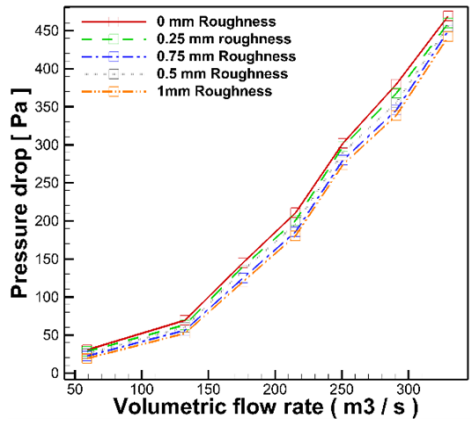


**Figure 7. Effects of Varying Volumetric Flow Rate Under Different Roughness Conditions on Pressure Drop**

## 4.2. Tangential Velocity

In general, internal flows in pipes or cyclonic flows, once the fluid flow transitions from laminar and transitional to turbulent flow, their velocity profiles within the pipe or gas cyclones no longer change, and they continue their path with essentially constant velocity. In the gas flow inside gas cyclones, the hydrodynamic flow behaves such that the flow, using either the tangential or axial channel, gains initial acceleration through centrifugal force, causing the flow to adopt a sweeping and tangential pattern along the walls. In fluids, there are generally two types of vortices that are important in internal flows. The primary vortex is a free vortex that usually forms along the walls. However, as the flow approaches the cyclone wall, the intensity of the gas's rotational flow decreases. This is primarily due to the gas boundary layer at the wall, where the viscous forces dominate over the diffusion forces, reducing and dissipating the fluid momentum. As a result, due to the no-slip condition at the cyclone walls, the velocity tends to approach zero, and the relationship can be expressed as follows:

$$V_t = \frac{C}{r} \tag{18}$$

However, in a forced vortex, due to the high rotation of the flow, the diffusion forces are able to overcome the viscous forces of the fluid. The relationship is linear, and the tangential velocity increases from the center of the cyclone toward the direction of the exit pipe. However, after reaching a maximum point, this value starts to decrease. The relationship for the free vortex is expressed as follows:

$$V_t = Cr \tag{19}$$

By combining both the forced vortex and the free vortex, a region is formed, which is referred to as the Rankine vortex. This is shown in (Figure 8).

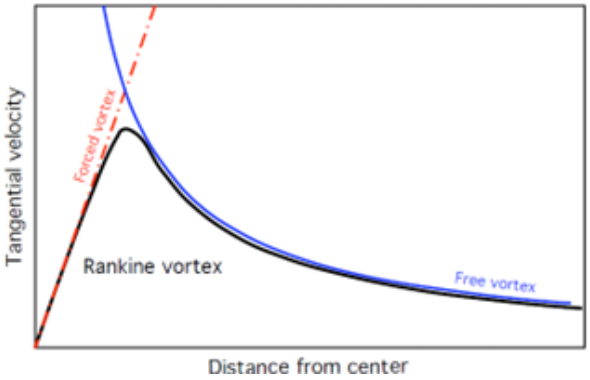


**Figure 8. Introduction of Vortex Regions in Tangential Velocity**

Considering the introduction of the hydrodynamic structure of tangential velocity in gas cyclones and inside pipes, this section discusses and examines the effects of wall roughness, which is crucial in the design, maintenance, and installation of gas cyclones. To investigate the effects of local roughness and observe the changes in tangential velocity along the radial direction, the entire computational domain of the axial gas cyclone is defined with four lines, as shown in the (Table 4).

**Table 4: Radial Positions in the Axial Cyclone Relative to the Coordinate System Center**

| $Z_1$ | $Z_2$ | $Z_3$ | $Z_4$ |
|---|---|---|---|
| 0 [mm] | 33 [ mm ] | 66 [ mm ] | 99 [ mm] |

As shown in (Figure 9), the tangential velocities exhibit an M-shaped distribution, indicating the effects of different wall roughness conditions. It can be observed that the tangential velocity decreases with increasing wall roughness. This decrease is due to the reduction in fluid momentum and its impact on the formation of small eddies near the wall, which in turn affects the larger eddies in the center of the axial gas cyclone. As seen, with increased wall roughness, the maximum tangential velocity, represented by the peaks in each of the graphs, decreases at specific positions. This reduction hinders the centrifugal force generated by the tangential velocity from effectively transferring or pushing the particles toward the cyclone wall, thereby disrupting the separation process. As a result, the efficiency of axial gas cyclones decreases with increased wall roughness. It is worth mentioning that the most critical section of a gas cyclone is the cylindrical section, as this is where the separation process primarily occurs, assuming there are no inhibiting factors. The conical section, on the other hand, plays a role in providing gravitational acceleration, which pushes the particles toward the lower section for accumulation.

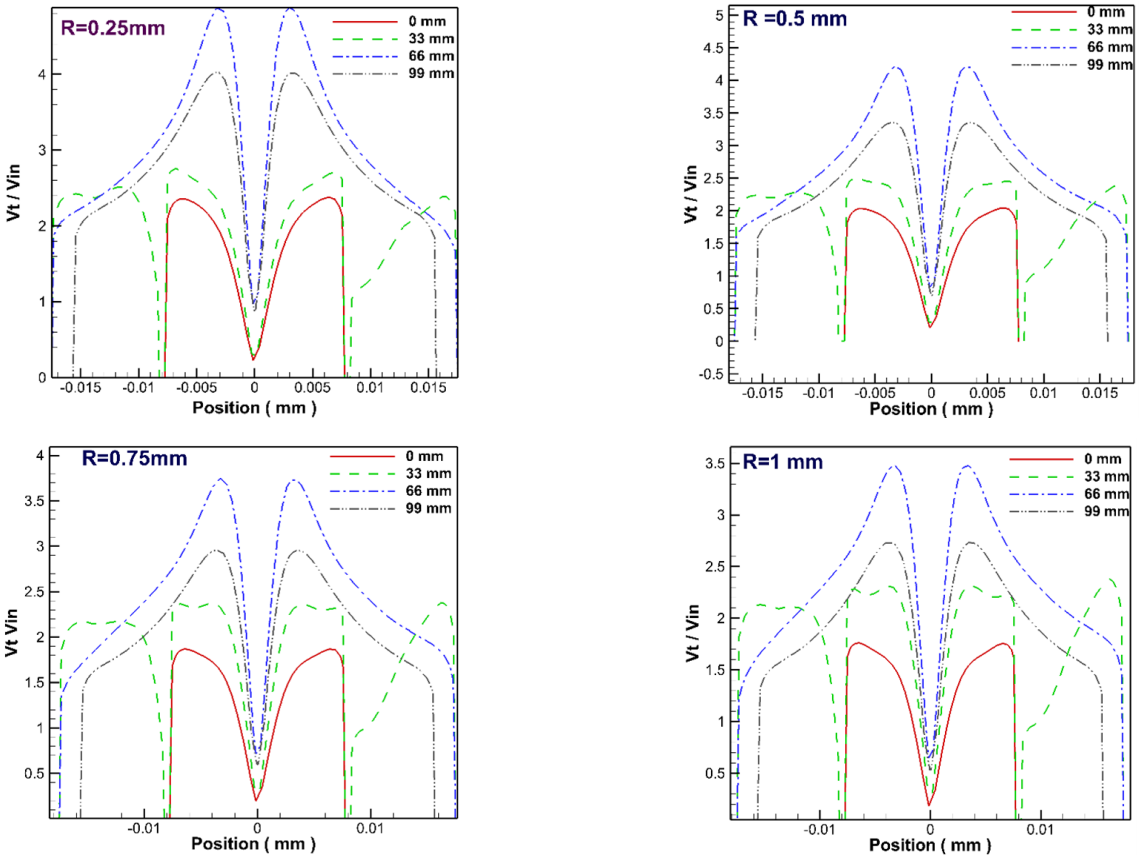


**Figure 9. Radial Distribution of Tangential Velocity with Different Roughness Conditions**

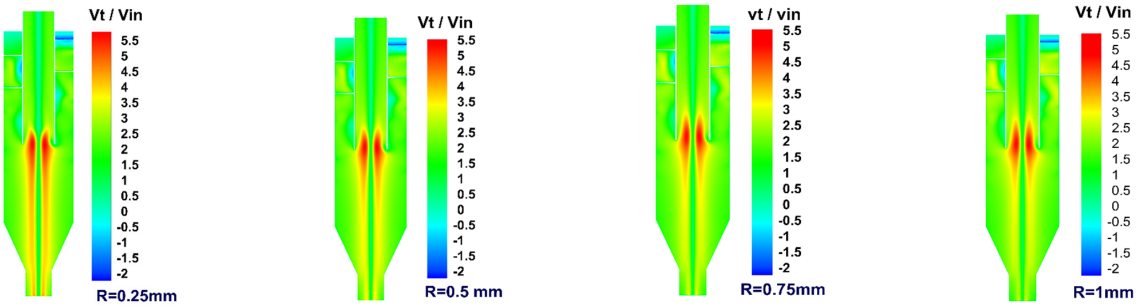


**Figure 10. Contours of Tangential Velocity at X=1 with a Velocity of 3.56 $m^2/s$**

As observed from the contours of tangential velocity shown in (Figure 10), the velocity increases in the baffle area due to the turbulence generated in the fluid. However, the roughness has a negative effect on the velocity in this region. On the other hand, the highest tangential velocity is found at the inlet of the exit pipe, as the flow undergoes a converging state, and the diameter of the exit pipe becomes smaller compared to the cyclone diameter, which leads to an increase in tangential velocity in this area. Up to this point, we have discussed the average tangential velocity, which plays a crucial role in the performance of the cyclone. However, in this section, the turbulent kinetic energy, which is related to the oscillatory velocities that lead to the transfer of momentum to the particles, will be discussed. As observed in (Figure 11), turbulent kinetic energy is directly related to the oscillatory velocities, as shown in Equation (20).

$$k = \frac{1}{2}\overline{u_i \acute{u}_j} \tag{20}$$

In (Figure 11), it can be observed that the location with the highest local velocity triggers oscillatory velocities in the turbulent gas flow, which in turn transfers additional momentum to the particles. As seen, at the inlet of the exit pipe, where the velocity is highest, the local turbulent kinetic energy is greater in this region compared to other areas. Therefore, with an increase in roughness, the momentum decreases, resulting in an inverse effect on the turbulent kinetic energy, which leads to the scattering of particles.

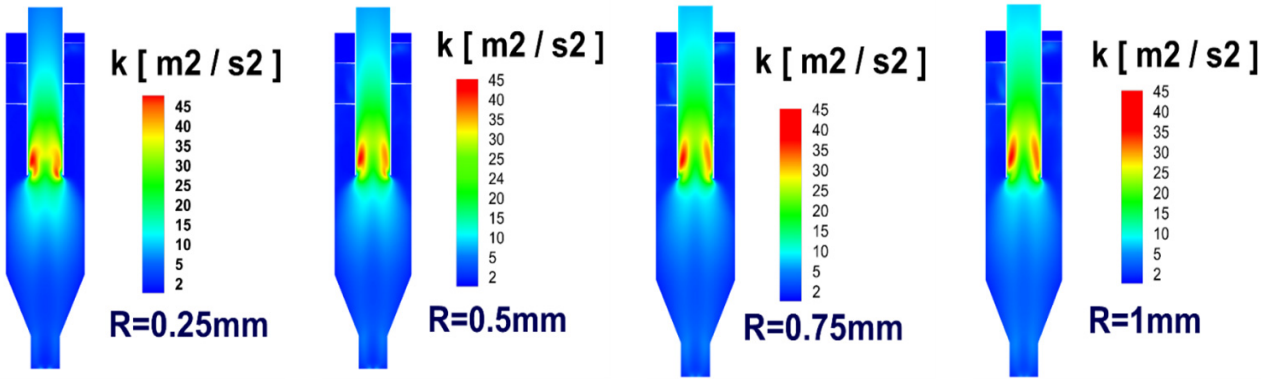


**Figure 11. Contours of Turbulent Kinetic Energy with Different Roughness Conditions at an Inlet Velocity of 3.56 m/s at Position X=1**

## 4.3. Axial Velocity

Particles vertically within the cyclone. It consists of two primary components: the downward axial flow, which carries gas and larger particles toward the conical section, and the upward flow through the central vortex, which guides finer particles toward the exhaust. Wall roughness influences axial velocity by altering near-wall momentum, particularly in the downward region where heavier particles tend to accumulate. Increased roughness reduces axial velocity near the walls due to added resistance, weakening the downward transport of coarse particles and potentially increasing their residence time. While the upward core flow is less directly impacted, the reduced tangential momentum and altered vortex strength (linked to roughness effects discussed in earlier sections) can disrupt the coherence of the upward flow as well. This, in turn, affects the evacuation of fine particles through the outlet. As shown in velocity contours (Figure 13), rougher walls lead to a noticeable decrease in axial flow near boundaries while maintaining relatively higher velocity in the vortex finder due to geometric convergence.

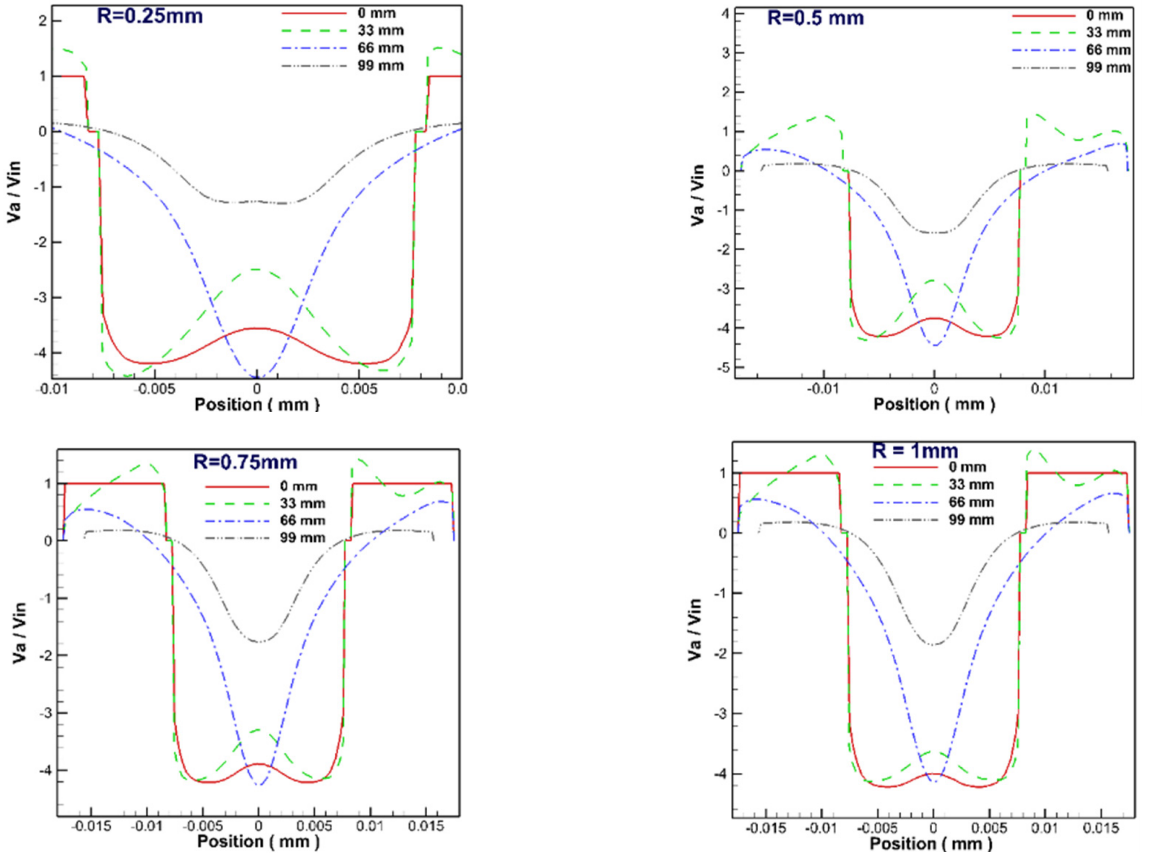


**Figure 12. Radial Positions of Axial Velocity**

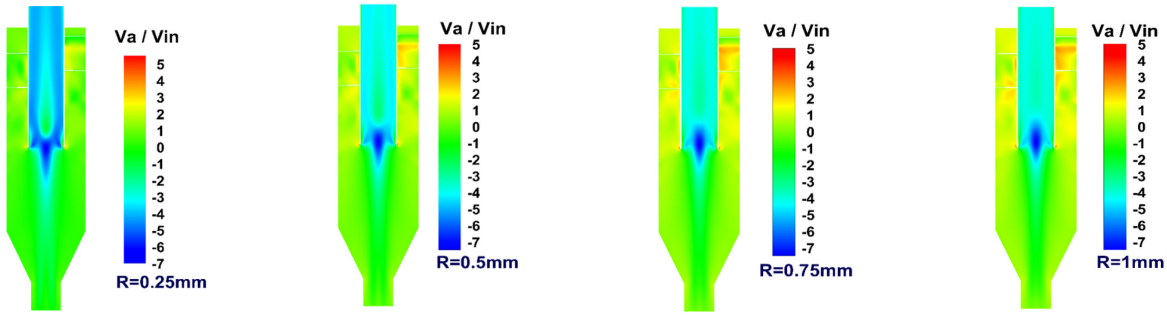


**Figure 13. Axial Velocity Contours with Different Roughness Conditions at a Velocity of 3.56 m/s (X=1)**

Overall, while axial velocity is not as dominant as tangential velocity in particle separation, its modulation by wall roughness significantly impacts flow stability, particle movement paths, and the balance between downward settling and upward escape, thereby influencing cyclone performance.

## 4.4. Efficiency of Axial Gas Cyclone

In general, for two-phase gas and particle flows in gas cyclones, the particle efficiency is obtained using the following relation:

$$\eta = \left(1 - \frac{n_{out}}{n_{total}}\right) \times 100 \quad (21)$$

In the above relation, $n_{out}$ represents the number of particles exiting the gas cyclone, and $n_{total}$ represents the total number of particles injected. The inlet velocity and even the configuration of the channel ends, gas inlet, and other geometric parameters such as cyclone diameter and inlet curvature angle are

interdependent in gas cyclones. Additionally, the particle material and even the material of the gas cyclone itself influence the cyclone's efficiency. Based on the hydrodynamic explanations provided in the sections on axial and tangential velocity, it can be observed that the effects of surface roughness and inlet velocity significantly influence this cyclone parameter, which is crucial in its design. Therefore, considering the results obtained from the effects of cyclone wall roughness along with variations in inlet velocity, as shown in (Figure 14), it can be concluded that increasing the inlet velocity improves the efficiency of the gas cyclone. As the inlet velocity increases, the tangential velocity and, consequently, the centrifugal force also increase, leading to higher efficiency and a reduction in the residence time of particles. This demonstrates that even the residence time of particles, which is related to their leakage, impacts the cyclone efficiency parameter.

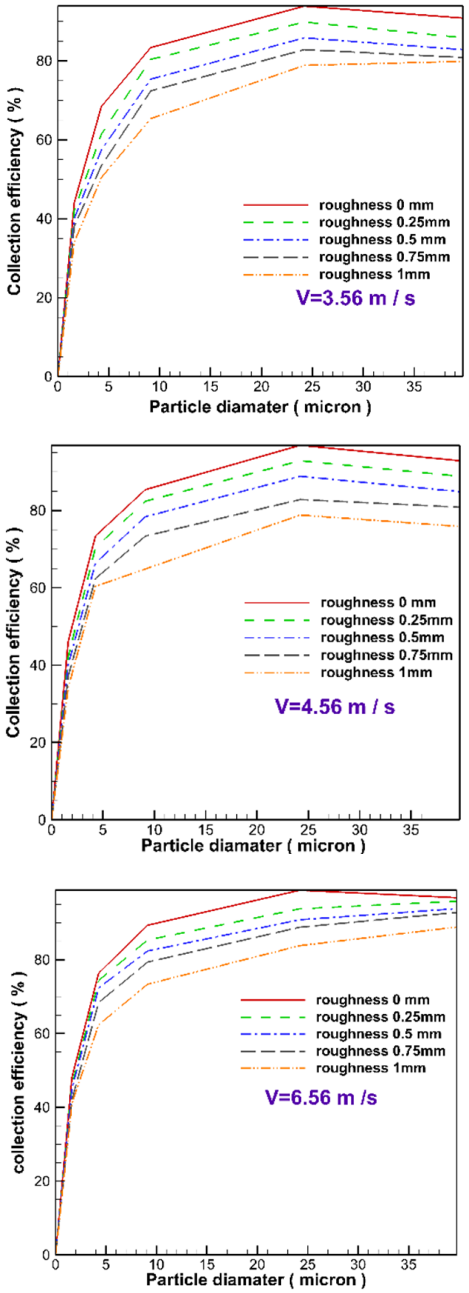


**Figure 14. Efficiency of the Axial Gas Cyclone under Different Roughness Conditions with Varying Inlet velocities**

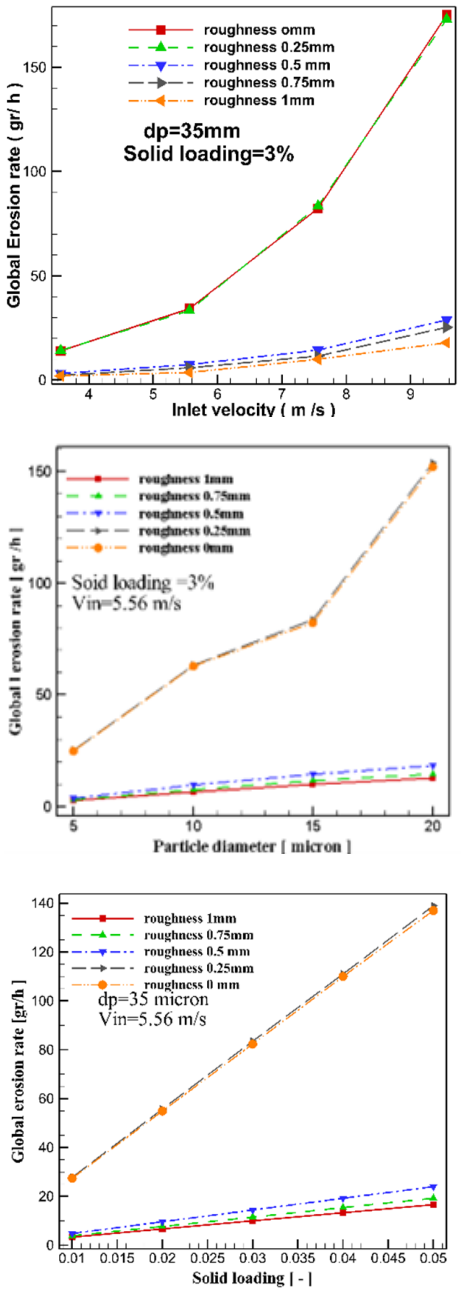


**Figure 15. Effects of Different Hydrodynamic Conditions with Applied Wall Roughness on Gas Cyclone Wall Erosion**

### 4.5. Gas Cyclone Wall Erosion

Wall erosion in gas cyclones is a critical durability concern, primarily caused by repeated impacts of solid particles on internal surfaces, particularly in high-velocity zones and at sharp directional changes in the flow. The erosion intensity depends on several factors, including particle size and concentration, gas velocity, impact angle, and the material properties of the cyclone wall. In this study, erosion is modeled using the Oka et al. (2005) approach to quantify material loss over time, with a specific focus on how wall roughness alters erosion behavior.

As demonstrated in (Figures 15 and 16), increased wall roughness leads to a measurable reduction in erosion rate. This occurs because rough surfaces disrupt high-speed particle trajectories, decreasing the frequency and severity of direct impacts—especially in critical regions such as the cone tip, where particle convergence is highest due to the flow's spiral and gravitational patterns. While high inlet velocities and large particle sizes still contribute to some degree of erosion, rough walls tend to diffuse particle motion and reduce radial pressure buildup near the surface, which collectively lowers localized stress. Moreover, the reduction in tangential and axial velocities observed in roughened configurations (as previously discussed) also translates to lower kinetic energy transfer during collisions, thereby enhancing mechanical durability. Although roughness may slightly compromise separation efficiency, its benefits in prolonging cyclone lifespan—by mitigating wall thinning and structural fatigue—make it a key factor in long-term cyclone design optimization. This trade-off underscores the importance of balancing aerodynamic performance with physical wear resistance when evaluating modifications such as surface treatments, coatings, or structural reinforcements in industrial cyclone applications.

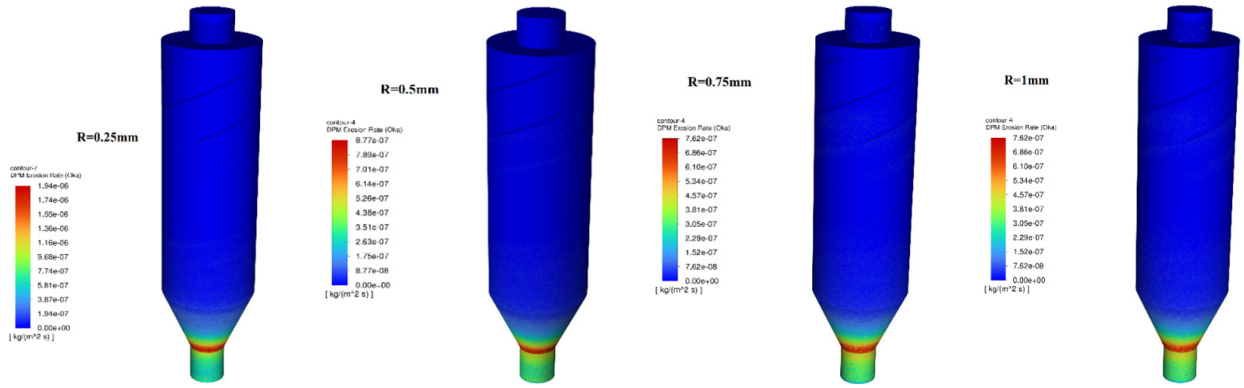


**Figure 16. 3D Contours of Particle Erosion Rate at a Velocity of 3.56 m/s**

To further validate the findings of this study, a comparison with relevant recent research is provided in (Table 5) The comparative analysis focuses on pressure drop, separation efficiency, and wall erosion behavior under varying wall roughness conditions and operating parameters.

**Table 5: Comparison this Study with Other Studies**

| Study | Year | Focus | Pressure Drop | Collection Efficiency | Erosion Modeling | Notable Features |
|---|---|---|---|---|---|---|
| This study | 2025 | Axial cyclone with wall roughness | ↓ 9% (with increased roughness) | ↓ up to 12% (for >25 µm) | Included | Full CFD + RSM + erosion + DPM |
| Li et al. | 2023 | Outlet tube optimization | ↓ 6% | ↑ 5-8% | Not included | Geometric tuning only |
| Babaoğlu et al. | 2023 | Geometry + acoustic control | Not reported | ↑ 10% | Not included | Focus on noise & shape |
| Foroozesh et al. | 2021 | Surface roughness impact | ↓ 8% | ↓ 10% | Included | Similar setup, limited velocity range |
| Kumar & Hassanpour | 2024 | Review on wall erosion | -- | -- | Included | Comprehensive review |
| Rahimi & Singh | 2025 | Axial cyclone geometry optimization | ↓ %7.5 | ↑ %9-6 | Not included | Applied response surface modeling |

## 5. Conclusions

This study presents a comprehensive numerical investigation into the impact of wall roughness on flow behavior, pressure drop, separation efficiency, and erosion rate in axial gas cyclones. Using an integrated modeling approach—combining Reynolds Stress Model (RSM), Discrete Phase Modeling (DPM), and advanced erosion modeling—this work offers a detailed understanding of fluid-particle interactions under various roughness conditions. One of the key innovative aspects of this study is the simultaneous evaluation of aerodynamic performance and mechanical durability, which is often neglected in prior research. While previous works have primarily focused on geometric optimizations or performance metrics in isolation, this research highlights the trade-off between reduced pressure drop (≈9%) and lower separation efficiency (≈12% for particles >25 µm), while also showing a significant reduction in wall erosion (≈15%) due to increased roughness. Unlike many existing studies that do not incorporate erosion modeling or high-resolution turbulence approaches, our work provides a more holistic and realistic perspective on cyclone design. By emphasizing the dual role of wall roughness and validating results against experimental and literature data, this study contributes a valuable framework for optimizing axial cyclone designs. It bridges a critical gap in the literature by addressing not only flow performance but also long-term durability, offering practical insights for industrial applications where both efficiency and equipment lifespan are crucial.

## References

Austrheim, T. (2006). Experimental characterization of high-pressure natural gas scrubbers, PhD thesis, University of Bergen.

Brar, L. S., Sharma, R. P., & Elsayed, K., 2015. The effect of the cyclone length on the performance of Stairmand high-efficiency cyclone. Powder Technology, 286, 668-677. https://doi.org/10.1016/j.powtec.2015.09.003.

Brar, L. S., & Elsayed, K., 2017. Analysis and optimization of multi-inlet gas cyclones using large eddy simulation and artificial neural network. Powder Technology, 311, 465-483. https://doi.org/10.1016/j.powtec.2017.02.004.

Brar, L. S., & Elsayed, K., 2018. Analysis and optimization of cyclone separators with eccentric vortex finders using large eddy simulation and artificial neural network. Separation and Purification Technology, 207, 269-283. https://doi.org/10.1016/j.seppur.2018.06.013

Babaoğlu, N. U., Parvaz, F., Hosseini, S. H., Elsayed, K., & Ahmadi, G., 2021. Influence of the inlet cross-sectional shape on the performance of a multi-inlet gas cyclone. Powder Technology, 384, 82-99. https://doi.org/10.1016/j.powtec.2021.02.008

Babaoğlu, N. U., Parvaz, F., Foroozesh, J., Hosseini, S. H., Ahmadi, G., & Elsayed, K., 2023. Geometry optimization of axial cyclone for high performance and low acoustic noise. Powder Technology, 427, 118738. https://doi.org/ 10.1016/j.powtec.2023.118738

Deng, Y., Yu, B., & Sun, D., 2020. Multi-objective optimization of guide vanes for axial flow cyclone using CFD, SVM, and NSGA II algorithm. Powder Technology, 373, 637-646. https://doi.org/10.1016/j.powtec.2020.06.078

Dehdarinejad, E., Bayareh, M., Parvaz, F., Hosseini, S. H., & Ahmadi, G., 2023. Performance analysis of a gas cyclone with a converging-diverging vortex finder. Chemical Engineering Research and Design, 193, 587-599. https://doi.org/10.1016/j.cherd.2023.04.012

Elsayed, K., & Lacor, C., 2010. Optimization of the cyclone separator geometry for minimum pressure drop using mathematical models and CFD simulations. Chemical Engineering Science, 65(22), 6048-6058. https://doi.org/10.1016/j.ces.2010.08.042

Elsayed, K., Parvaz, F., Hosseini, S. H., & Ahmadi, G., 2020. Influence of the dipleg and dustbin dimensions on performance of gas cyclones: An optimization study. Separation and Purification Technology, 239, 116553. https://doi.org/10.1016/j.seppur.2020.116553

Foroozesh, J., Parvaz, F., Hosseini, S. H., Ahmadi, G., Elsayed, K., & Babaoğlu, N. U., 2021. Computational fluid dynamics study of the impact of surface roughness on cyclone performance and erosion. Powder Technology, 389, 339-354. https://doi.org/10.1016/j.powtec.2021.05.041

Gimbun, J., Chuah, T. G., Choong, T. S., & Fakhru'l-Razi, A., 2005. Prediction of the effects of cone tip diameter on the cyclone performance. Journal of Aerosol Science, 36(8), 1056-1065. https://doi.org/10.1016/j.jaerosci.2004.10.014

Hsiao, T. C., Chen, D., Greenberg, P. S., & Street, K. W., 2011. Effect of geometric configuration on the collection efficiency of axial flow cyclones. Journal of Aerosol Science, 42(2), 78-86. https://doi.org/10.1016/j.jaerosci.2010.11.004

Hsu, Y. D., Chein, H. M., Chen, T. M., & Tsai, C. J., 2005. Axial flow cyclone for segregation and collection of ultrafine particles: theoretical and experimental study. Environmental science & technology, 39(5), 1299-1308. https://doi.org/10.1021/es0491735

Huang, L., Deng, S., Chen, Z., Guan, J., & Chen, M. (2018). Numerical analysis of a novel gas-liquid pre-separation cyclone. Separation and Purification Technology, 194, 470-479. https://doi.org/10.1016/j.seppur.2017.11.050

Karagoz, I., & Kaya, F. (2007). CFD investigation of the flow and heat transfer characteristics in a tangential inlet cyclone. International Communications in Heat and Mass Transfer, 34(9-10), 1119-1126. https://doi.org/10.1016/j.icheatmasstransfer.2007.05.017

Kaya, F., Karagoz, I., & Avci, A. (2011). Effects of

surface roughness on the performance of tangential inlet cyclone separators. Aerosol science and technology, 45(8), 988-995. https://doi.org/10.1080/02786826.2011.574174

Kumar, D., & Hassanpour, A. (2024). Recent advances in cyclone separator modeling: A review on wall roughness and erosion. Powder Technology, 432, 118945. https://doi.org/10.1016/j.powtec.2023.118945

Li, J., Wang, T., Zhang, L., Chang, J., Song, Z., & Ma, C. (2020). Multi-objective optimization of axial-flow-type gas-particle cyclone separator using response surface methodology and computational fluid dynamics. Atmospheric Pollution Research, 11(9), 1487-1499. https://doi.org/10.1016/j.apr.2020.06.002

Li, W., Huang, Z., & Li, G. (2023). Improvement of the cyclone separator performance by the wedge-shaped roof: A multi-objective optimization study. Chemical Engineering Science, 268, 118404. https://doi.org/10.1016/j.ces.2023.118404

Li, M., Zhao, Y., & Chen, W. (2024). A comparative study on the effect of wall surface coatings on erosion in industrial cyclones. Chemical Engineering Journal, 465, 142387. https://doi.org/10.1016/j.cej.2023.142387

Liu, G., Wang, W., Yu, J., & Li, X. (2022). Effect of extra inlets structure on cyclone wall erosion. Powder Technology, 411, 117926. https://doi.org/10.1016/j.powtec.2022.117926

Mao, Y., Pu, W., Zhang, H., Zhang, Q., Song, Z., Chen, K., & Han, D. (2019). Orthogonal experimental design of an axial flow cyclone separator. Chemical Engineering and Processing-Process Intensification, 144, 107645. https://doi.org/10.1016/j.cep.2019.107645

Morsi, S. A. J., & Alexander, A. J. (1972). An investigation of particle trajectories in two-phase flow systems. Journal of Fluid mechanics, 55(2), 193-208. https://doi.org/10.1017/S0022112072001806

Ogawa, A., Iwanami, T., & Shono, H. (1997). Estimation of the collection efficiency of the axial flow cyclone dust collector with the fixed guide vanes. Journal of Thermal Science, 6, 58-65. https://doi.org/10.1007/s11630-997-0017-2

Oka, Y. I., Okamura, K., & Yoshida, T. (2005). Practical estimation of erosion damage caused by solid particle impact: Part 1: Effects of impact parameters on a predictive equation. Wear, 259(1-6), 95-101. https://doi.org/10.1016/j.wear.2005.01.039

Oka, Y. I., & Yoshida, T. (2005). Practical estimation of erosion damage caused by solid particle impact: Part 2: Mechanical properties of materials directly associated with erosion damage. Wear, 259(1-6), 102-109. https://doi.org/10.1016/j.wear.2005.01.040

Parvaz, F., Hosseini, S. H., Ahmadi, G., & Elsayed, K. (2017). Impacts of the vortex finder eccentricity on the flow pattern and performance of a gas cyclone. Separation and Purification Technology, 187, 1-13. https://doi.org/10.1016/j.seppur.2017.06.045

Parvaz, F., Vahedi, S. M., & Khandan, M. (2018). Numerical investigation of the effects of geometry variation on the flow pattern and performance of Gas-Particle cyclones. Iranian Journal of Mechanical Engineering Transactions of ISME, 19(4), 101-122. https://doi.org/10.22060/ijme.2018.14439.5724

Parvaz, F., Rafee, R., & Talebi, F. (2018). Effects of the Outlet Pipe Diameter on the Performance of Aerocyclone in Gas Droplet Two-Phase Flow. https://doi.org/10.1016/j.cep.2019.107645

Parvaz, F., Hosseini, S. H., Elsayed, K., & Ahmadi, G. (2018). Numerical investigation of effects of inner cone on flow field, performance and erosion rate of cyclone separators. Separation and Purification Technology, 201, 223-237. https://doi.org/10.1016/j.seppur.2018.03.030

Parvaz, F., Hosseini, S. H., Elsayed, K., & Ahmadi, G. (2020). Influence of the dipleg shape on the performance of gas cyclones. Separation and Purification Technology, 233, 116000. https://doi.org/10.1016/j.seppur.2019.116000

Parvaz, F., Hosseini, S. H., Bastan, A. R., Foroozesh, J., Babaoğlu, N. U., Elsayed, K., & Ahmadi, G. (2023). Influence of gas exhaust geometry on flow pattern, performance, and erosion rate of a gas cyclone. Korean Journal of Chemical Engineering, 40(7), 1587-1597. https://doi.org/10.1007/s11814-023-1430-2

Rahimi, A., & Singh, P. (2025). CFD-based optimization of axial cyclone geometry for dual-phase separation. Journal of Fluids Engineering, 147(3), 031501. https://doi.org/10.1115/1.4054932

Vahedi, S. M., Parvaz, F., Kamali, M., & Jafari Jebeli, H. (2018). Numerical investigation of the impact of inlet channel numbers on the flow pattern, performance, and erosion of gas-particle cyclone. Iranian Journal of Oil and Gas Science and Technology, 7(4), 59-78. https://doi.org/10.22050/ijogst.2018.16066.1300

Vahedi, S. M., Parvaz, F., Rafee, R., & Khandan Bakavoli, M. (2018). Computational fluid dynamics simulation of the flow patterns and performance of conventional and dual-cone gas-particle cyclones. Journal of Heat and Mass Transfer Research, 5(1), 27-38. https://doi.org/10.22075/jhmtr.2017.11918.1170

Vahedi, S. M., Parvaz, F., Khandan Bakavoli, M., & Kamali, M. (2020). Effect of Surface Roughness on Vortex Length and Efficiency of Gas-oil Cyclones through CFD Modelling. Iranian Journal of Oil and Gas Science and Technology, 9(1), 68-84. https://doi.org/10.22050/ijogst.2020.19460.1543

Xiong, Z., Ji, Z., & Wu, X. (2014). Development of a cyclone separator with high efficiency and low pressure drop in axial inlet cyclones. Powder Technology, 253, 644-649. https://doi.org/10.1016/j.powtec.2013.12.016

Zhang, S., Shin, M., & Shin, W. G. (2021). Comparison of models to predict the collection efficiency of an axial cyclone with a spindle vane. Journal of Aerosol Science, 157, 105817. https://doi.org/10.1016/j.jaerosci.2021.105817

# تأثیر زبری دیواره بر الگوی جریان و عملکرد سیکلون گازی محوری به همراه نرخ فرسایش


- مسعود درفشان[1*]، ستار مقدم[2]، فرزاد پرواز[3]

۱. استادیار، گروه مهندسی مکانیک، دانشکده فنی و مهندسی، دانشگاه صنعتی خاتم‌الانبیا بهبهان، بهبهان، ایران

۲. دانشجو کارشناسی ارشد، گروه مهندسی مکانیک، دانشکده فنی و مهندسی، دانشگاه صنعتی خاتم الانبیا بهبهان، بهبهان، ایران

۳. کارشناسی ارشد، گروه مهندسی مکانیک، دانشکده فنی و مهندسی، دانشگاه سمنان، سمنان، ایران

(ایمیل نویسنده مسئول: dorfeshan@bkatu.ac.ir)


## چکیـــــــده


در این مطالعه، تأثیر زبری دیواره بر الگوی جریان، عملکرد و نرخ فرسایش در یک سیکلون گازی محوری بررسی شده است. سیکلون‌های گازی به دلیل انعطاف‌پذیری، هزینه‌های نگهداری پایین و کارایی در کنترل آلودگی هوا، به‌طور گسترده در صنایع مختلف مانند فرآوری مواد غذایی، خشک‌کن‌ها و صنعت سیمان برای جداسازی ذرات جامد از جریان گاز استفاده می‌شوند. مدل‌سازی عددی با استفاده از مدل‌های آشوبناکی، مدل‌های زبری سطح، مدل فاز گسسته و مدل فرسایش انجام شده است تا پارامترهای کلیدی مانند افت فشار، سرعت مماسی، سرعت محوری، راندمان جداسازی و نرخ فرسایش دیواره تحلیل شوند. نتایج نشان می‌دهد که افزایش زبری دیواره باعث کاهش سرعت مماسی و در نتیجه کاهش نیروی گریز از مرکز می‌شود که این امر تأثیر منفی بر راندمان جداسازی ذرات دارد. از سوی دیگر، افزایش زبری دیواره منجر به کاهش افت فشار می‌شود که در طراحی سیکلون یک مزیت محسوب می‌گردد. تحلیل نرخ فرسایش نیز نشان می‌دهد که بیشترین فرسایش در بخش مخروطی پایین سیکلون رخ می‌دهد و افزایش زبری دیواره می‌تواند فرسایش را کاهش دهد. به‌طور کلی، این مطالعه نشان می‌دهد که زبری دیواره تأثیرات متضادی بر عملکرد سیکلون دارد—از یک سو افت فشار را کاهش می‌دهد و از سوی دیگر راندمان جداسازی را کم می‌کند؛ بنابراین، بهینه‌سازی زبری سطح برای دستیابی به تعادل بین این دو عامل در طراحی سیکلون‌های گازی محوری ضروری است. نتایج نشان داد که افزایش ناهمواری دیوار، سرعت مماسی را تا ۸۱ درصد کاهش داد، بازده جمع‌آوری سیکلون برای ذرات بزرگ‌تر از ۵۲ میکرومتر تقریباً ۲۱ درصد کاهش یافت، در حالی که افت فشار حدود ۹ درصد کاهش یافت که این موضوع در کاربردهای حساس به انرژی مفید محسوب می‌شود. بیشترین نرخ فرسایش در نوک مخروط سیکلون مشاهده شد و ناهمواری دیوار به کاهش میانگین فرسایش تقریباً ۵۱ درصد کمک کرد.


**واژگان کلیدی:** سیکلون گازی محوری، زبری دیواره، افت فشار، فرسایش دیواره، مدل فاز گسسته